Journal of Translational Medicine

RESEARCH

Open Access

Ferrostatin-1 reduces the inflammatory response of rheumatoid arthritis by decreasing the antigen presenting function of fibroblast-like synoviocytes

Xiaoying Zhu[1], Hanya Lu[1], Haonan Jia[1], Xuemin Wei[1], Jiawei Xue[1], Wenjing Li[1], Juan Zhang[1], Yanli Wang[1], Jingyao Yan[1], Haoyuan Sun[2], Yanlei Ge[3] and Zhiyi Zhang[1*]

Abstract

Rheumatoid arthritis (RA) is a systemic chronic autoimmune disease with complex mechanism. Currently, ferroptosis is believed to play a role in it, but the specific mechanism is unknown, especially in immune response. In this study, we demonstrated that the high expression of major histocompatibility complex I (MHC-I) molecules in RA fibroblast-like synoviocytes (FLSs) is an antigen-presenting cell property and that this property is closely related to the increase in antigens after citrullination. Moreover, we detected higher levels of ferroptosis among FLSs from RA patient than among FLSs from OA patients. Ferroptosis can increase the expression of citrullinated histone H3 (cit-h3) by promoting the production of peptidyl arginine deiminase 4 (PAD4), which further promotes the expression of MHC-I molecules. We cocultured RA-FLSs treated with ferroptosis drugs with selected CD8 + T cells to assess the effect of ferroptosis on the endogenous antigen-presenting function of RA-FLSs. Ferroptosis promoted the proliferation of CD8 + T cells and the release of the inflammatory factors Tumor necrosis factor-α (TNF-α) and Interferon-gamma (IFN-γ), which enhanced the inflammatory effect. This phenomenon was also observed in a collagen-induced arthritis (CIA) mouse model. Finally, ferrostatin-1 (fer-1), a ferroptosis inhibitor, inhibited the above effects and reduced the release of inflammatory factors, indicating that ferroptosis may play a therapeutic role in RA and providing new ideas for the treatment of RA in the field of immunity.

Keywords Rheumatoid arthritis, Ferroptosis, Immune, Antigen presentation, Inflammation

*Correspondence:
Zhiyi Zhang
zhangzhiyi2014@163.com
[1]Department of Rheumatology, First Affiliated Hospital of Harbin Medical University, Harbin, China
[2]Department of Osteology, Heilongjiang Provincial Hospital, Harbin, China
[3]Department of Respiratory Medicine, North China University of Science and Technology Affiliated Hospital, Tangshan, China

Introduction

Rheumatoid arthritis (RA) is one of the most common chronic systemic inflammatory diseases, with joint destruction as its most characteristic clinical manifestation. This destruction is driven by chronic inflammation, immune and stromal cell activation, and synovial cell layer invasion into adjacent cartilage and underlying bone. Phenotypic changes in synovial cells play crucial roles in this process [1, 2]. During the activation of the autoimmune response, synovial cells are believed to undergo significant proliferation and exhibit invasive and destructive behaviours, further promoting inflammation. The inflammatory environment, in turn, accelerates synovial proliferation and destructive effects, creating a positive feedback loop [3, 4]. Additionally, under the stimulation of inflammatory factors, synovial fibroblasts can exhibit antigen-presenting functions, thereby enhancing the inflammatory response [5–7].

Citrullination is the posttranslational modification of arginine in proteins to the nonstandard amino acid citrulline; this modification is catalysed by a calcium ion-dependent PAD enzyme [8]. Protein citrullination can produce new epitopes that lead to the formation of new autoantigens; the modified protein has stronger immunogenicity and increased uptake by antigen-presenting cells [9]. Citrullination is currently considered a marker of early cell damage; thus, it appears to be involved in all cell death pathways [10].

Ferroptosis is an iron-dependent form of programmed cell death characterized by the accumulation of iron ions and lipid peroxides [11]. This phenomenon was discovered in 2012 by Brent Stockwell's laboratory at Columbia University while studying the role of the small molecule compound erastin in tumour mutation mechanisms [12]. Ferroptosis primarily occurs due to the depletion of glutathione (GSH) and the inactivation of glutathione peroxidase 4 (GPX4), with GPX4 identified as a key inhibitory factor [11]. Numerous studies have revealed the involvement of ferroptosis in the development of various diseases, including tumours, kidney diseases, and cardiovascular diseases [13–16]. However, researchers have focused mostly on the effects of cell death induced by ferroptosis, while the potential amplification of inflammatory diseases through the accumulation of reactive oxygen species (ROS) remains underexplored. Although ferroptosis is closely related to immune-inflammatory mechanisms and plays a role in the development of immune diseases [17–19], no studies have yet been conducted in the context of RA.

Therefore, in this study, we focused on the influence of changes in the microenvironment inside cells on the citrullination mechanism in RA during ferroptosis, which led to the enhancement of the antigen-presenting function of synovial fibroblasts and a series of inflammatory effects, and further explored the mechanism of ferroptosis in RA. Based on this theory, we found that ferroptosis inhibitor can effectively inhibit the inflammatory response of RA.

Materials and methods

OA and RA patients

The samples for this study were obtained from patients with osteoarthritis (OA) and rheumatoid arthritis (RA) who attended the Rheumatology and Immunology Department and Orthopedic Outpatient and Inpatient Departments of the First Affiliated Hospital of Harbin Medical University. The diagnoses of RA and OA were made according to the criteria established by the American College of Rheumatology in 2010 [20] and 1991 [21]. A total of 24 RA patients were included for peripheral blood collection to sort CD8 + T cells. All patients had positive CCP antibodies, and all belonged to patients with moderate and severe disease activity. In addition, 20 patients who underwent joint replacement and synovial clearance in our department of Orthopedics were included for the extraction of FLSs. All patients had no other chronic or joint diseases and were not treated with disease-modifying anti-rheumatic drugs (DMARDs), but could be treated with oral NSAIDs.

This study was approved by the Ethics Committee of the First Affiliated Hospital of Harbin Medical University, and informed consent was obtained from all patients (NO. 2025JS17).

Cell isolation and cell culture

Peripheral blood mononuclear cells (PBMCs) from RA patients were isolated using density gradient centrifugation. CD8 + T cells were separated using an EasySep™ Human CD8 + T Cell Isolation Kit (Stemcell Technologies) following the manufacturer's instructions. The sorted cells were seeded at a density of 1×10^6 cells/mL in 6-well plates and stimulated with a CD3/CD28/CD2 T cell activator (25 μL/mL; Stemcell Technologies) and IL-2 (100 U/mL, MCE) in RPMI-1640 medium (Biological Industries) supplemented with 10% heat-inactivated foetal bovine serum (FBS; Gibco).

RA fibroblast-like synoviocytes (FLSs) were isolated from the synovium of RA patients undergoing joint replacement surgery. The specific methods were described in a previous publication by the corresponding author [22]. The cells were cultured in Dulbecco's modified Eagle's medium (DMEM) supplemented with 10% FBS. Adherent FLSs were passaged at a ratio of 1:3 when they reached 70–80% confluence and were used for experiments at passages 4 to 7. Serum starvation was performed for 24 h in DMEM containing 1% FBS before treatment.

RA FLSs were treated with or without the ferroptosis activator erastin (0, 2.5, 5, or 7.5 μM, MCE) or the ferroptosis inhibitor fer-1 (0, 5, 10, or 15 μM, MCE) for 48 h. The PAD4 enzyme inhibitor GSK484 (10 μM, MCE) was added to the erastin-containing medium. Cells were cultured for 6 h.

Coculture of synovial cells and CD8 + T cells

For cocultures, 1×10^5 T cells were cocultured with RA-FLS target cells at a 1:1 ratio in one well of a 6-well culture plate. Prior to coculture, RA-FLSs were extensively washed to remove residual drug. After 48 h, the T cells were stained for CFSE, IFN-γ, TNF-α, and CD8 expression for flow cytometric analysis.

Flow cytometry

For the intracellular staining of CD8 + T cells, APC-TNF-α (BioLegend) and PE-IFN-γ (BioLegend) were used, while for surface staining, FITC-CD8a (BioLegend) and PE/Cy7-CD69 (BioLegend) were used. Nuclear staining was performed with a secondary antibody (goat anti-rabbit IgG (H + L) FITC-conjugated, 1:500, Abcam) labelled with anti-cit-h3 (1:500, Abcam). APC-CD8a and FITC-CFSE (BioLegend) were used to assess CD8 + T cell proliferation. FLSs were stained with C11BODIPY581/591 (BODIPY) and FITC-HLA A2 (BioLegend). Briefly, for surface staining, after treatment, cells were collected and resuspended in ice-cold PBS containing 3% FBS and a primary antibody. Following a 25-min incubation on ice and protected from light, the cells were washed twice, resuspended in ice-cold PBS, and analysed using a BD FACSCalibur (BD Biosciences, New Jersey, USA). For intracellular staining, the cells were incubated with appropriate concentrations of cell stimulants and blockers (BioLegend) for 4–5 h in a cell culture incubator (37 °C, 5% CO_2), fixed and permeabilized. The cells were subsequently stained according to the aforementioned steps. Nuclear staining was performed according to the manufacturer's instructions for the True-Nuclear™ Transcription Factor Buffer Set (BioLegend). Data analysis was performed using FlowJo software (Tree Star, USA).

Collagen-induced arthritis (CIA) mouse model

Male DBA/1J mice (8 weeks old, weighing 21 ± 2 g, SPF, SLAC, Jiangsu, China) were selected to establish a CIA model. The CIA mouse model was established as previously described [23]. In brief, 2 g/L bovine type II collagen (CII, Chondrex, Redmond, WA, USA) was emulsified in an equal concentration of complete Freund's adjuvant (CFA) at a 1:1 ratio on ice, and 100 μL of the emulsion was injected into the base of the mouse tail to complete the first immunization. On day 21, prepared CII was emulsified with the same dose of incomplete Freund's adjuvant (IFA) and injected into the base of the mouse tail in the same manner to complete the second immunization. The general condition, weight, and degree of joint swelling of the mice were regularly monitored. After the CIA model was established (day 21), the mice were randomly divided into the following groups (each group consisted of 5 mice): CIA control group; erastin group [CIA model mice treated with erastin at a dose of 5 mg/kg/day; intraperitoneal injection one week before and two weeks after the second immunization, twice a week for a total of 6 times); fer-1 group (CIA model mice treated with fer-1 at a dose of 10 mg/kg/day according to the aforementioned dosing regimen); and erastin + GSK484 group (intraperitoneal injection of 10 mg/kg, three times a week for a total of 6 times, starting two weeks after the second immunization). All the animal experiments were conducted following the Guidelines for the Care and Use of Laboratory Animals of the National Institutes of Health and were approved by the Institutional Animal Care and Use Committee of Harbin Medical University (NO. 2022076). Specimen providers and data statisticians were blinded to the group allocation.

Real-time quantitative polymerase chain reaction (RT–qPCR)

Total RNA was extracted from FLSs using an RNA Kit (Omega), and reverse transcription was performed using ReverTra Ace® qPCR RT Master Mix with gDNA Remover (TOYOBO) according to the manufacturer's protocol. The generated complementary DNA (cDNA) served as the template for qPCR amplification, which was conducted using iTaq Universal SYBR Green Supermix (Bio-Rad). The gene primers used are listed in supplementary Table 1. Gene expression was normalized to that of GAPDH using the $2^{-\Delta\Delta Ct}$ method.Specimen providers and data statisticians were blinded to the group allocation.

Western blot analysis

After digestion with Accutase (Solarbio), the FLSs were washed with PBS. The FLSs were subsequently lysed in cold lysis buffer with rotation every 10 min for a total of 30 min. Subsequently, the lysates were centrifuged, and the supernatants were collected. The samples were then heated at 95 °C for 10 min in loading buffer. Protein extracts containing 30 μg of protein were separated via 10% SDS–PAGE and transferred onto NC membranes. Western blot analysis was performed using primary antibodies against HLA Class I (1:5000, Proteintech), PAD4 (1:5000, Proteintech), GPX4 (1:1000, Abcam), and either GAPDH or α-tubulin, followed by secondary antibodies conjugated to horseradish peroxidase (HRP), such as goat anti-rabbit IgG or anti-mouse IgG (1:5000, Abbkine). The results were visualized using an Odyssey CLx Infrared Imaging System.

Specimen providers and data statisticians were blinded to the group allocation.

ELISA

After drug treatment, the cells were washed with sterile PBS and cocultured with an equal volume of medium containing CD8 + T cells. The supernatant was collected for ELISAs. The detection of IFN-γ (Jianglai Bioscience) and TNF-α (Jianglai Bioscience) was performed according to the manufacturer's instructions.Specimen providers and data statisticians were blinded to the group allocation.

Histological and immunohistochemistry analysis

The hind paws of mice were fixed in 10% neutral buffered formalin, decalcified in 10% EDTA for 3 weeks, and then embedded in paraffin wax. Sections were prepared from tissue blocks and stained with haematoxylin and eosin. Histological scoring of joint inflammation, synovial hyperplasia and bone erosion were performed as described previously [24, 25]. Immunostaining was conducted using the following primary antibodies: anti-HLA class I (Proteintech), anti-PAD4 (Proteintech), anti-GPX4 (Abcam) and anti-CD8 (Abcam).

Microcomputed tomography (micro-CT) imaging

We employed microcomputed tomography (micro-CT) imaging technology using the Quantum GX system from Perkin Elmer, Waltham, USA, to reconstruct the hind paws of the mice into three-dimensional (3D) bone structures, enabling the observation of joint damage. To assess bone loss, we utilized Caliper Analyze software (Analyze Direct, Kansas, USA) to calculate the average CT value.

Statistical analysis

All analyses were completed using GraphPad Prism 10 (GraphPad Prism Software, CA, USA). The data are presented as means ± S.D.s. Paired *t* tests were used to compare the two groups. The Mann–Whitney U test was applied for data with nonnormal distributions. For the analysis of differences between groups, one-way ANOVA or two-way ANOVA was used depending on the number of groups and the nature of the comparisons. *P* values < 0.05 were considered significant. $^{*}P < 0.05$, $^{**}P < 0.01$, $^{***}P < 0.001$, and $^{****}P < 0.0001$.

Results

Elevated levels of ferroptosis in synovial cells from RA patients

RA is characterized primarily by synovial inflammation. Changes in the synovial cells of affected joints most directly reflect the pathogenesis of RA. To assess the levels of ferroptosis in RA, we measured the expression of the ferroptosis marker GPX4 in synovial cells from RA patients using PCR and Western blotting (WB). The results indicated a significant decrease in GPX4 expression in RA synovial cells (Fig. 1a and b). Using the C11-BODIPY probe and flow cytometry, we assessed intracellular lipid peroxidation levels, which were significantly increased in RA patients (Fig. 1c). Additionally, fluorescence microscopy revealed increased ferrous ion and reactive oxygen species (ROS) levels in the synovial cells of RA patients (Fig. 1d and e). These findings collectively suggest that ferroptosis levels are greater in the synovial cells of RA patients than in those of osteoarthritis (OA) patients.

Antigen-presenting characteristics of synovial cells from RA patients

RA is characterized by the significant presence of citrullinated antigens. Using citrullinated histone H3 as a representative marker, we found markedly greater citrullinated histone H3 levels in RA fibroblast-like synoviocytes (RA-FLSs) than in osteoarthritis fibroblast-like synoviocytes (OA-FLSs) (Fig. 1i). These modified antigens have a relatively high affinity for MHC molecules. To determine whether synovial cells from RA patients can function as antigen-presenting cells and promote inflammation in synovial tissue, we assessed the expression of HLA class I antigens in RA-FLSs via Western blotting (WB). Additionally, we used flow cytometry and PCR to analyse HLA-A2 expression levels. Compared with those in OA-FLSs, the levels of both genes in RA-FLSs were significantly greater (Fig. 1f-h). These findings suggest that the increased presence of citrullinated antigens in RA promotes the expression of MHC class I molecules in RA-FLSs and facilitates the transformation of RA-FLSs into an antigen-presenting cell phenotype.

Ferroptosis affects HLA class I molecule expression in RA-FLSs

To delve into the role of ferroptosis in RA, we initially investigated the cytotoxic effects of various concentrations of the ferroptosis inducer erastin and the ferroptosis inhibitor Fer-1 on synovial cells. The CCK-8 assay revealed a dose-dependent increase in erastin-induced cytotoxicity in RA-FLSs. Notably, there was no significant difference in cytotoxicity between 10 and 15 μM fer-1, with survival rates surpassing 50% across all the tested concentrations (Supplementary Fig. 1a and b).

To gauge the responsiveness of ferroptosis markers to different drug concentrations, we evaluated GPX4 expression via PCR and WB. The results revealed that erastin robustly inhibited GPX4 expression at relatively high concentrations, while fer-1 tended to increase GPX4 mRNA levels, although protein levels decreased at 15 μM fer-1 (Supplementary Fig. 1d-g).

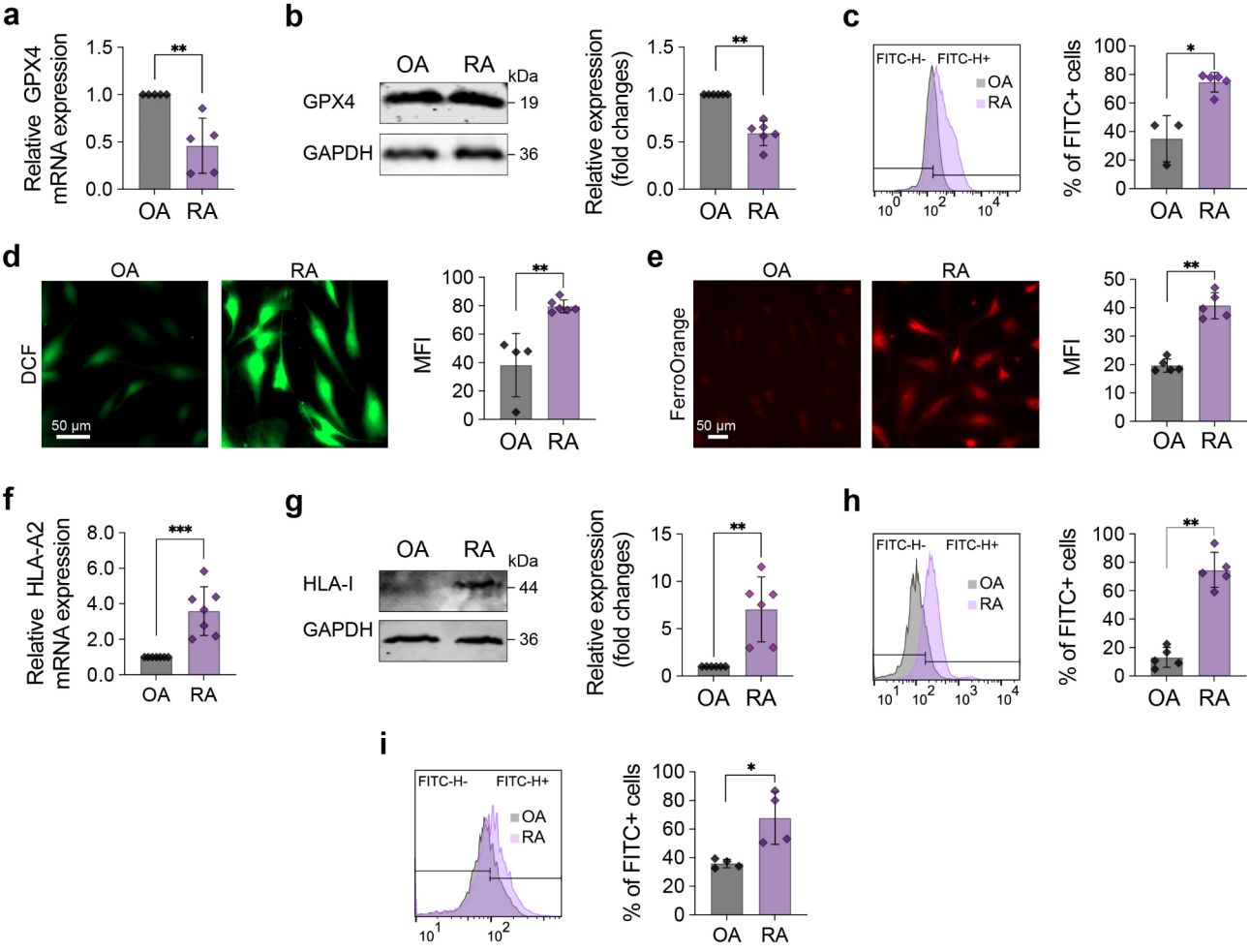

Fig. 1 Ferroptosis and increased MHC-I levels in rheumatoid arthritis
(**a, b**) qPCR and WB analyse the expression of GPX4 in FLSs and the statistical result of the relative fold values (normalized the OA control group) ($n=5$–6); (**c**) Flow cytometry analysis of FLSs after staining with 1 μM C11-BODIPY$^{581/591}$ ($n=3$–5); (**d**) Immuno-fluoresence of FLSs stained for DCFH-DA and the statistical result of mean fluorescence intensity (MFI) ($n=4$–6); (**e**) Immuno-fluoresence of FLSs stained for FerroOrange (green) and the statistical result of mean fluorescence intensity (MFI) ($n=5$); (**f, g**) qPCR and WB analyse the expression of HLA-I in FLSs and the statistical result of the relative fold values (normalized the OA control group) ($n=6$–7); (**h**) Flow cytometry analysis the expression of HLA-A2 in FLS($n=5$); (**i**) Flow cytometry analysis the expression of cit-h3 in FLSs ($n=4$); Data are shown as the mean ± S.D.; Each dot plot represents an individual sample; All data were statistically analyzed using Mann-Whitney U test. *$P<0.05$, **$P<0.01$, ***$P<0.001$

To explore the interplay between elevated ferroptosis levels in RA patients and synovial cell antigen-presenting molecules, we investigated the impact of varying erastin and fer-1 concentrations on MHC class I molecules. All erastin concentrations increased the surface expression of MHC class I on RA-FLSs, with 5 μM resulting in the most potent effect ($P<0.05$, Fig. 2a-c). Conversely, 10 μM fer-1 had the most pronounced inhibitory effect on MHC class I expression ($P<0.05$, Fig. 2d and e), with flow cytometry corroborating similar inhibition at 10 and 15 μM fer-1 (Fig. 2f).

Ferroptosis affects the production of citrullinated histone H3 by PAD4 enzyme

Ferroptosis can cause RA-FLSs to express MHC-I molecules. We explored whether this effect is related to an increase in citrullinated antigens. The generation of citrullinated proteins requires the catalytic action of PAD enzymes. Therefore, we examined the expression of the PAD4 enzyme under different concentrations of ferroptosis-inducing drugs. The results indicated that 5 μM erastin significantly promoted PAD4 expression (Fig. 2g), whereas Fer-1 inhibited PAD4 expression, with the strongest effect at 10 μM (Fig. 2h). Thus, we propose that ferroptosis promotes the generation of citrullinated proteins by increasing PAD4 enzyme production.

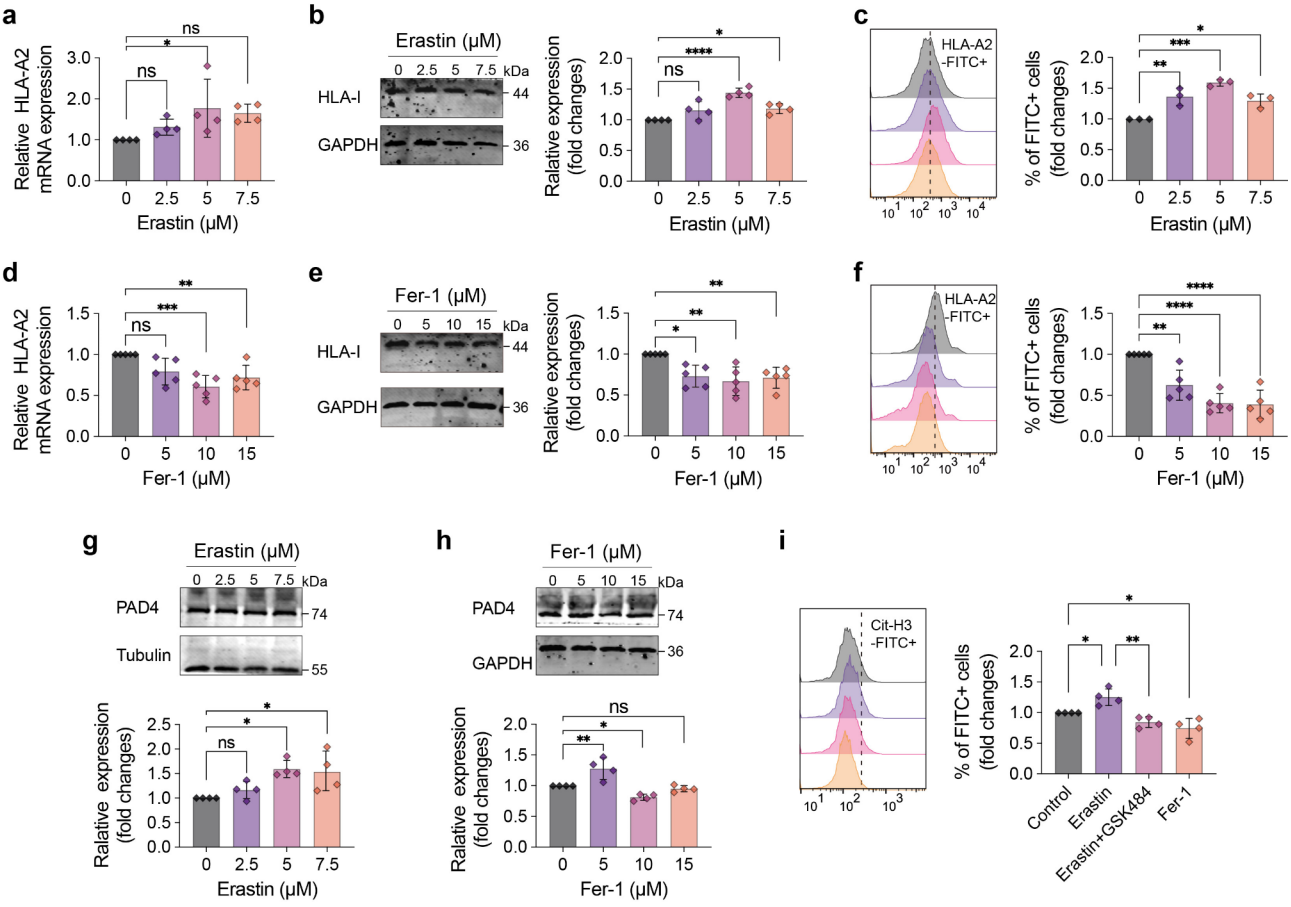

Fig. 2 Effect of ferroptosis on citrullinated histone H3 and HLA-A2 in RA-FLSs via PAD4

Analyse the expression of HLA-I in FLSs that treatment with 0μM, 2.5μM, 5μM,7.5μM erastin for 48 h by: (**a, b**) qPCR and WB analyse ($n=4$); (**c**) Flow cytometry ($n=3$); Analyse the expression of HLA-I in FLSs that treatment with 0, 5, 10,15 μM fer-1 for 48 h by: (**d, e**) qPCR and WB analyse ($n=5$); (**f**) Flow cytometry ($n=5$); (**g, h**) qPCR and WB analyse the expression of PAD4 in FLSs that treatment with 0, 2.5, 5, 7.5 μM erastin and 0, 5, 10,15 μM fer-1 for 48 h ($n=4$); (**i**) Flow cytometry analysis the expression of cit-h3 in FLSs that treatment with 5 μM erastin,10 μM fer-1 for 48 h and 5 μM erastin for 48 h combine with 10 μM GSK484 for 6 h (add after the effect of erastin has ended) ($n=4$); All statistical results are expressed as relative folded values (normalized the untreated control group). The dotted line in the histogram represent the reference lines for statistical positive percentage. Data are expressed as mean ± S.D. Each dot plot represents an individual sample; For statistical analysis, one-way ANOVA followed by Dunnett's method for multiple comparisons. *$P<0.05$; **$P<0.01$, ***$P<0.001$, ****$P<0.0001$

On the basis of the cytotoxicity data, ferroptosis marker expression, and MHC-I expression under different concentrations of erastin and fer-1, we determined that the optimal concentrations of erastin and fer-1 were 5 μM and 10 μM, respectively. Flow cytometry analysis confirmed that erastin promotes the generation of cit-h3, which can be inhibited by the PAD4 enzyme inhibitor GSK484, whereas fer-1 inhibits the generation of cit-h3 (Fig. 2i).

Ferroptosis influences the antigen presentation function of RA-FLSs via the PAD4 enzyme, thereby further impacting the release of inflammatory factors

To investigate the mechanism by which ferroptosis enhances antigen presentation in RA-FLSs, we treated the cells with erastin and the PAD4 inhibitor GSK484 and then measured HLA-I levels. We found that the erastin-induced increase in HLA-I was inhibited by GSK484 (Fig. 3a-c). The effect of GSK484 on cell viability is shown in Supplementary Fig. 1c.

Next, we cocultured RA-FLSs with CD8 + T cells. Using flow cytometry, we examined the expression of the CD8 + T cell activation markers CD69, TNF-α, and IFN-γ. The results revealed that the levels of activation markers of CD8 + T cells significantly increased after coculture with RA-FLSs, although they were still lower than those after stimulation with IL-2 and CD3/CD28/CD2, a finding that was in line with expectations. Because the extracted CD8 + T cells were highly individualized, we classified the coculture group as 1 and calculated the correlation between the positive control group and this group. Although the stimulatory function of RA-FLSs could not be directly explained, the percentage of RA-FLSs in the coculture group was not significantly different

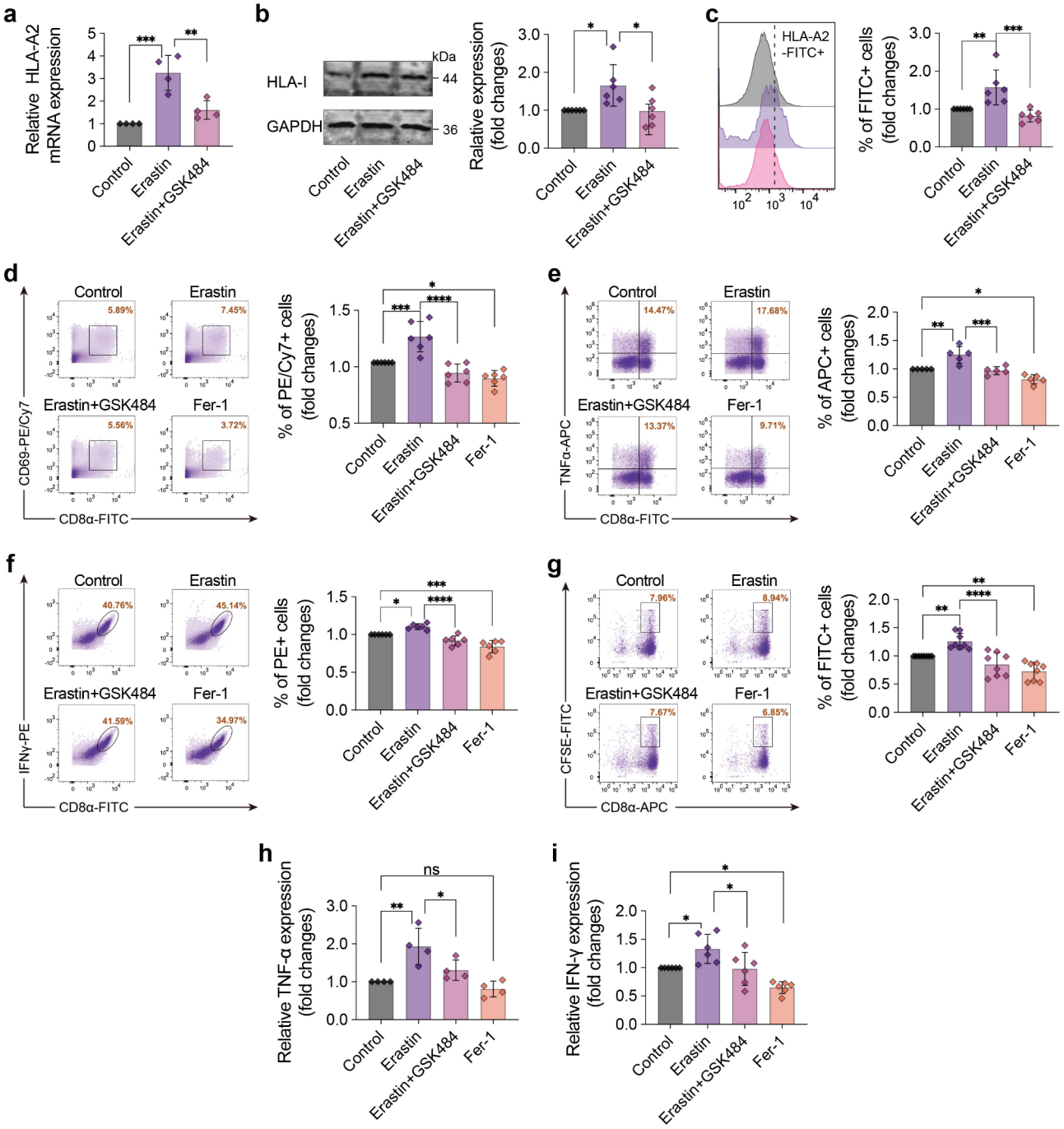

Fig. 3 Ferroptosis Promotes Antigen Presentation in RA-FLSs through PAD4 Enzyme, however, ferroptosis inhibitor fer-1 inhibits antigen presentation and reduce inflammatory cytokine release

(**a, b**) qPCR and WB analyse the expression of HLA-I in FLSs that treatment with different drugs ($n=4$–6); (**c**) Flow cytometry analysis the expression of HLA-A2 in FLSs that treatment with different drugs($n=6$); (**d-f**) CD8 + T cells were purified from CCP + RA patients and co-cultured with RA-FLSs without additional stimul for 48 h. RA-FLSs need to be stimulated by different drugs and then participate in co-culture. Representative flow cytometric images of CD8 + T cells and percentage of (**d**) CD69 + cells($n=6$) (**e**) TNF-α + cells ($n=5$) (**f**) IFN-γ + cells ($n=6$); (**g**) CD8 + T cells purified from CCP + RA patients were labeled with 1 μM CFSE for 5 min at RT in PBS and then PBS containing 10%FCS was added to halt the reaction. Labeled CD8 + T cells were co-cultured with RA-FLSs without additional stimul for 48 h. RA-FLSs need to be stimulated by different drugs and then participate in co-culture. Flow cytometry analysis the percentage of cells labeled with CFSE ($n=8$); (**h, i**) Collect the cell supernatant after co-culture. ELISA analyse the expression of TNF-α and IFN-γ in supernatant ($n=4$–6); The FLSs need to treat with different drugs as follow: 5 μM erastin for 48 h, 10 μM fer-1 for 48 h and 5 μM erastin for 48 h combine with 10 μM GSK484 for 6 h (add after the effect of erastin has ended). All statistical results are expressed as relative folded values (normalized the untreated control group). The dotted line in the histogram represent the reference lines for statistical positive percentage. Data are expressed as mean ± S.D. Each dot plot represents an individual sample; For statistical analysis, one-way ANOVA followed by Dunnett's method for multiple comparisons. *$P<0.05$; **$P<0.01$, ***$P<0.001$,****$P<0.0001$

from that in the positive control group according to the polyclonal stimulation data of the positive control group. We added a group of unstimulated CD8 + T cells as a blank control, but the cells had poor survival ability in vitro. Surprisingly, the cells in the coculture group grew normally. The same trend was observed for cell proliferation as determined by CFSE staining (Supplementary Fig. 2a-d). In addition, the content of inflammatory factor protein in the cell supernatant of CD8 group alone, FLS group alone and co-culture group was detected by ELISA, and it was found that the sum of inflammatory factors in the two separate culture groups was much lower than that in the co-culture group (Supplementary Fig. 2e and f). Therefore, we speculate that RA-FLSs can significantly stimulate the activation of CD8 + T cells. T cell activation marker expression increased with erastin treatment and was inhibited by GSK484, whereas they decreased with fer-1 treatment (Fig. 3d-f). CFSE staining further revealed that CD8 + T cell proliferation followed a similar trend (Fig. 3g).

Additionally, ELISAs of the coculture supernatant confirmed the same patterns for TNF-α and IFN-γ levels, providing further evidence of the antigen-presenting function of RA-FLSs in RA, a phenomenon associated with ferroptosis levels (Fig. 3h and i).

In summary, fer-1, an ferroptosis inhibitor, can effectively inhibit the endogenous antigen presenting function of RA-FLSs and reduce the release of inflammatory factors. The mechanism may be related to the effect of ferroptosis on PAD4 enzyme.

Ferroptosis influences joint inflammation and damage through PAD4 in a CIA mouse model

Previous in vitro experiments demonstrated that the levels of ferroptosis can influence antigen presentation function in RA-FLSs. To explore that finding, we constructed a CIA mouse model and administered intraperitoneal injections of erastin, fer-1, or GSK484. The paws of mice in the CIA group exhibited significant swelling compared with those of mice in the NC group, with inflammation scores reaching arthritis levels. Erastin exacerbated paw inflammation, which was inhibited by GSK484, and fer-1 reduced inflammation. Additionally, erastin increased paw thickness, an effect inhibited by GSK484, and fer-1 reduced paw thickness (Fig. 4b and c).

Micro-CT revealed that erastin exacerbated bone destruction in the paws, as strongly reflected by a decrease in calcification in images. This damage was inhibited by GSK484, and Fer-1 alleviated bone destruction (Fig. 4d). HE staining results revealed that CIA led to inflammatory cell infiltration, synovial hyperplasia, and local joint damage. The erastin group exhibited extensive inflammatory cell infiltration, with proliferating synovial tissue markedly invading the articular cartilage and causing joint surface destruction. Cotreatment with GSK484 slightly alleviated these symptoms, whereas Fer-1 significantly reduced them (Fig. 5a-d).

In summary, ferroptosis aggravated joint inflammation and damage in a CIA mouse model, however, fer-1 inhibited the progression of arthritis in CIA mouse models and played a therapeutic role. The effects could be blocked by modulating the PAD4 enzyme.

Ferroptosis influences antigen presentation and inflammatory response in CIA mice via the production of PAD4 and citrullinated histone H3

Previous findings demonstrated the role and mechanism of ferroptosis in enhancing antigen presentation functions in RA-FLSs. To determine whether ferroptosis influences antigen-presenting function in the synovial tissue of CIA mice and promotes inflammation, we examined the expression of MHC-I and CD8. The erastin group presented significant increases in MHC-I and CD8 expression levels, which were reduced in mice cotreated with GSK484; conversely, the fer-1 group showed marked inhibition (Fig. 5e), suggesting that ferroptosis triggers endogenous antigen presentation in synovial cells, recruiting many CD8 + T cells.

Furthermore, we assessed the expression of cit-h3 and PAD4. Erastin promoted the expression of both genes, an effect that was decreased by GSK484, whereas fer-1 inhibited the expression cit-h3 and PAD4. Finally, the results of the immunohistochemical analysis of the TNF-α and IFN-γ levels were consistent with our in vitro experiments (Fig. 5e).

In summary, our results indicate that RA-FLSs possess antigen-presenting capabilities, contributing to proinflammatory effects. Ferroptosis affects cit-h3 expression in RA-FLSs via PAD4 regulation, leading to the change of HLA-I (MHC-I) molecules and antigen presentation-induced inflammation.

Discussion

Rheumatoid arthritis (RA) is a prevalent autoimmune disease, and previous research has focused primarily on immune cells and cytokines involved in its pathogenesis [1]. The initiation of autoimmune responses in RA starts with T cells recognizing self-antigens presented by antigen-presenting cells (APCs). Synovial cells, crucial effectors in RA, also exhibit nonprofessional antigen-presenting capabilities [2, 26]; however, their role in antigen presentation within RA remains incompletely understood, emphasizing the importance of identifying the factors that activate these cells.

Synovial cells in RA undergo phenotypic changes, resulting in the adoption of an aggressive phenotype [27]. These alterations include metabolic shifts (e.g., glycolysis) and the secretion of proinflammatory cytokines,

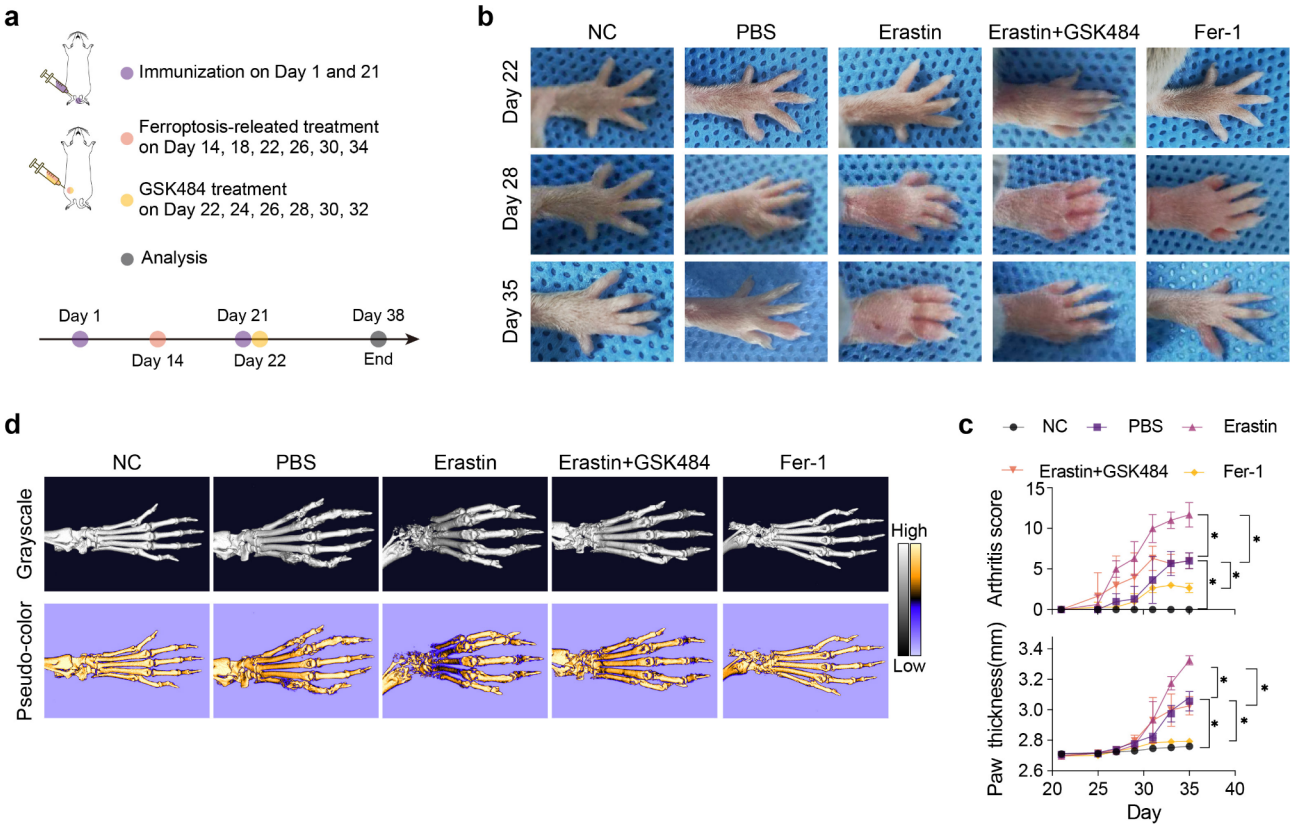

Fig. 4 Effects of ferroptosis on joint inflammation and bone destruction in CIA mice
(**a**) illustration of CIA mouse model therapy in vivo; (**b**) Representative photography of the hind limb from mice taken on day 22, day 28 and day 35; (**C**) Arthritis score and paw thickness evaluated from day 20 to day 35; (**d**) Representative micro-computed tomography (micro-CT) images; NC = normal control. PBS = CIA mice group; Erastin = CIA mice treated with erastin group. Fer-1 = CIA mice treated with fer-1 group. Erastin + GSK484 = CIA mice treated with erastin and GSK484 group. Data are expressed as mean ± S.D. For statistical analysis, one-way ANOVA followed by Dunnett's method for multiple comparisons. *$P < 0.05$; **$P < 0.01$, ***$P < 0.001$,****$P < 0.0001$

stimulating synovial fibroblasts to adopt a proinflammatory and tissue-destructive phenotype and thereby exacerbating RA [3]. The genetic predisposition to RA involves single nucleotide polymorphisms (SNPs) in immune regulation genes [28, 29], such as HLA-DRB1, peptidyl arginine deiminase type IV (PADI4), and protein tyrosine phosphatase, nonreceptor type 22 (PTPN22) [30]. Notably, the HLA-DRB1 region of MHC-II is particularly implicated in seropositive RA patients [31]. Therefore, scholars have focused on the response of CD4 + T cells. Studies have shown that in addition to directly damaging joint tissue, synovial fibroblasts can express costimulatory factors characteristic of APCs, activating MHC-II-restricted T cell hybridomas specific for arthritogenic peptides [5]. This is in line with the theoretical hypothesis.

In contrast to previous findings, we focused on the environmental changes inside FLSs during the occurrence of ferroptosis, which are mainly triggered by endogenous antigen presentation. So we mainly detected the changes of endogenous antigen presentation marker HLA-I. Our study revealed that RA-FLSs exhibit increased expression of MHC-I molecules, which is supported by multiple experimental findings indicating a significant increase in HLA-A2 expression. Citrullinated antigens, crucial post-translationally modified antigens in RA, play a significant role in the diagnosis of RA [32]. These antigens fit snugly into the binding grooves of SE-containing HLA-DR proteins, facilitating antigen presentation to T cells [33]. We speculate that RA-FLSs may harbour more endogenous citrullinated antigens than OA-FLSs do, potentially leading to increased MHC-I molecules, a topic that warrants further investigation.

In our study, we assessed the levels of cit-h3, a representative citrullinated protein that is believed to be correlated with RA disease activity [34]. Our results revealed significantly higher cit-h3 levels in RA-FLSs than in control FLSs, providing additional support for our hypothesis.

Moreover, we observed a greater level of ferroptosis in RA-FLSs, exacerbating the onset of RA, which differs from the results of some investigators. Ferroptosis is a newly identified iron-dependent cellular demise mechanism characterized by the accumulation of lipid

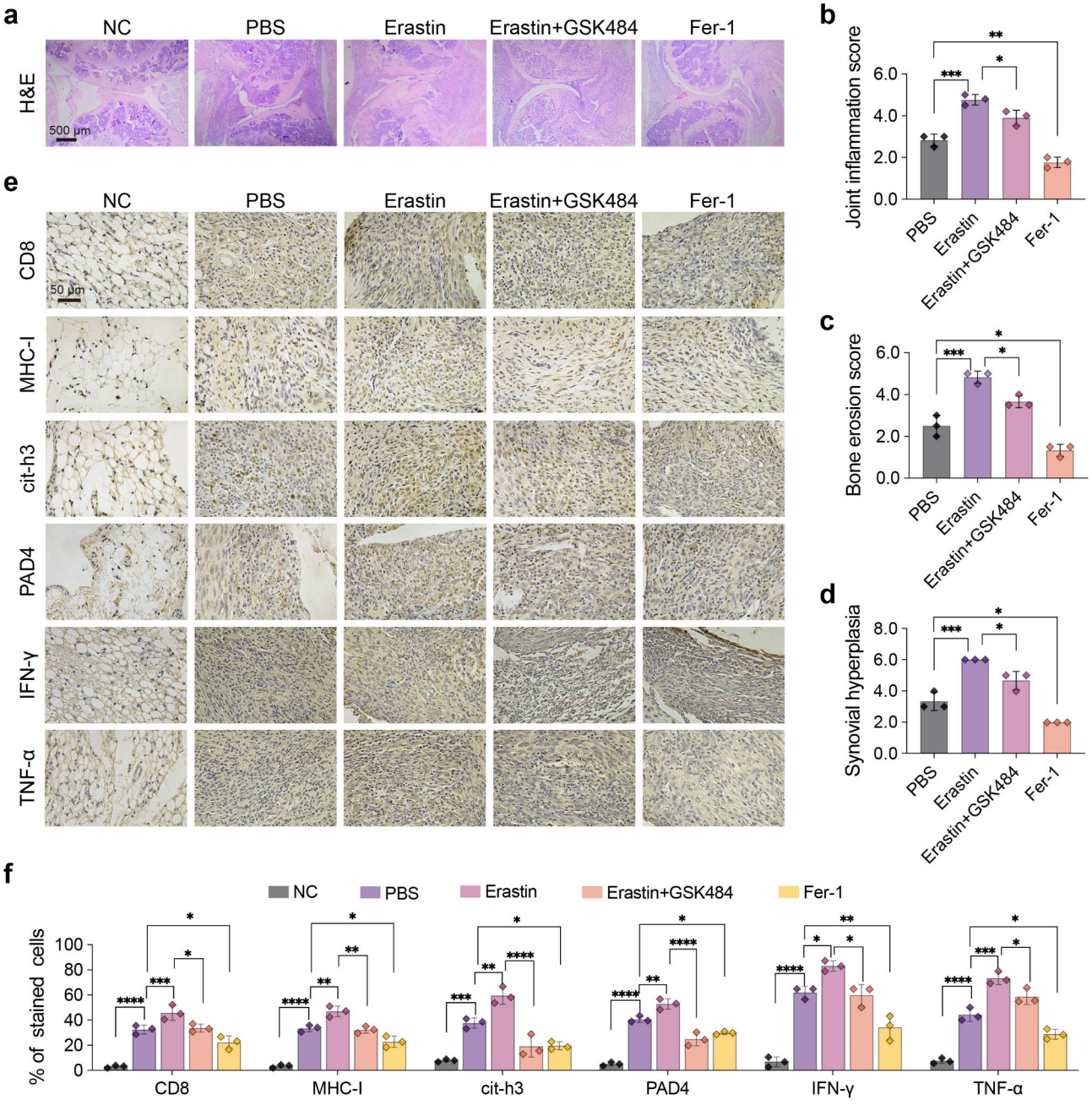

Fig. 5 Effects of ferroptosis on citrullinated antigens, endogenous antigen presenting markers and inflammatory factors
(**a**) Image of hematoxylin and eosin staining of hind knee joint; (**b-d**) Histological scores of joint inflammation, synovial bone erosion and hyperplasia; (**e-f**) Representative immunohistochemical staining of CD8, MHC-I, cit-h3, PAD4, TNF-α and IFN-γ and quantitative analysis of the percentage of positive cells. ($n = 3$); NC = normal control; PBS = CIA mice group; Erastin = CIA mice treated with erastin group. Fer-1 = CIA mice treated with fer-1 group. Erastin + GSK484 = CIA mice treated with erastin and GSK484 group. Data are expressed as mean ± S.D. Each dot plot represents an individual sample; For statistical analysis, one-way ANOVA followed by Dunnett's method for multiple comparisons. *$P < 0.05$; **$P < 0.01$, ***$P < 0.001$, ****$P < 0.0001$

reactive oxygen species (ROS) [35]; however, its role in RA is controversial. Notably, from the perspective of the tumour-like behaviour of RA-FLSs, fostering ferroptosis effectively mitigates the proliferation and invasion of RA-FLSs [36]. However, ferroptosis results in significant ROS production, leading to an imbalance in oxidative stress, which can escalate the inflammatory state of RA-FLSs and contribute to bone destruction [37]. Our in vivo findings suggest that erastin can stimulate proliferation and inflammatory responses in the synovium of CIA model mice, contradicting the observations of Jiao Wu et al. [38]. Nonetheless, in their study, erastin was administered at a dosage four times greater than that used in our study. Hence, we speculate that a high erastin dosage may

induce FLS death, curtailing the release of inflammatory factors in the synovium, whereas a low dosage of erastin primarily triggers inflammation through ROS accumulation, which is consistent with the results reported by Chen Zhao et al. [39].

Previous findings highlighted an increase in citrullinated proteins in RA. Peptidylarginine deiminases (PADs) catalyse the citrullination of arginine residues in protein peptide chains [8]. Among the PAD family members, PAD2 and PAD4 are notably abundant in the synovium and play pivotal roles in RA pathogenesis [40]. Anti-PAD4 antibodies are linked with severe joint damage [41, 42], whereas anti-PAD2 antibodies are associated with milder joint damage and lung disease in RA patients [43]. Additionally, autoantibodies in RA patients exhibit a greater affinity for PAD4-citrullinated fibrinogen than for PAD2 [44, 45]. Given that our tissue samples were sourced from patients with severe joint damage necessitating joint replacement, we identified PAD4 as the primary factor driving increased citrullinated protein levels in our study. Furthermore, PAD4-mediated histone citrullination plays a crucial role in neutrophil extracellular trap (NET) formation, with PAD4 exhibiting the closest association with histones [46], which partly explains our selection of cit-h3 as a representative citrullinated protein.

During instances of abnormal cell death, PAD enzymes may undergo abnormal activation, leading to heightened levels of protein citrullination [47, 48]. Consequently, we hypothesize that during ferroptosis, the abnormal activation of PAD enzymes results in the increased expression of citrullinated proteins, thereby enhancing antigen presentation in RA-FLSs. However, how does ferroptosis trigger the upregulation of PAD enzyme expression? PADs are typically inactive under normal physiological conditions, and PAD activity is calcium dependent. However, PAD activity can be induced under certain conditions, for example, high calcium levels, elevated bicarbonate concentrations, and specific redox conditions. Additionally, physiological injuries such as hypoxia and oxidative potassium neurotoxins can also impact PAD activity [49]. Consequently, we propose two mechanisms through which ferroptosis influences PAD4: (1) Ferroptosis leads to the accumulation of reactive oxygen species (ROS), causing peroxidation damage to cell membrane polyunsaturated fatty acids (PUFAs), which results in unrestricted extracellular influx of calcium ions, thereby triggering the abnormal activation of calcium-dependent PADs; (2) Ferroptosis induces an imbalance in oxidative stress. Our results indicate that different concentrations of erastin can stimulate PAD4 production, which supports our hypothesis. Fer-1 caused an increase in ROS levels at 5 μM and a significant decrease at 10 and 15 μM. Considering that small doses of fer-1 caused a decrease in ROS levels, the cell interior was more inclined towards a reduced state, which was conducive to the production of PAD4. However, with increasing concentration, the metabolic balance in the cell changed, and the redox state may have also changed. This triggered an inverse trend, which supports our hypothesis. The role of ferroptosis in RA is extremely complex, and deviations in the dose of a drug can lead to different effects but also different mechanisms of action.

Our results clearly revealed that ferroptosis activates the endogenous antigen presentation response in RA-FLSs. Additionally, we observed inflammatory factor activation in CD8 + T cells and detected inflammatory factor secretion into the supernatant. To increase the rigor of our experiment, considering the possibility that ferroptosis may also induce RA-FLSs to release inflammatory factors and that CD8 + T cells themselves can secrete such factors, we established separate groups of supernatants from cultures of RA-FLSs and CD8 + T cells alone. The results demonstrated that the total amount of inflammatory factors in the supernatants of these individual groups was significantly lower than that in the coculture groups, thus confirming our hypothesis (Supplementary Fig. 2e and f). These findings demonstrate that synovial cells indeed play a role in activating CD8 + T cells and that the role can be regulated by ferroptosis drugs. Moreover, this regulation can be blocked by PAD4 enzyme inhibitors.

In addition, there are still limitations in our study. First, regarding the selection of control group, since the extraction of synovium is an invasive operation and there is no obvious proliferating synovium in normal people, we chose the synovium of OA patients as the control group. However, due to the influence of various factors in OA (such as aging, metabolism, microinflammation, etc.), the normal control group still cannot be completely simulated. Nevertheless, we largely balanced certain factors during the case screening stage. Secondly, due to the limitation of sampling conditions for RA, the available synovium sample size is small, and primary FLSs are greatly affected by individual differences. Therefore, we need to expand the sample size to further verify our research results and increase the credibility of the data. Next, we will utilize FLSs as the target cells to further elucidate the mechanism by which ferroptosis affects citrullinated antigens, enhance our research on the process of antigen presentation and processing, thereby making this study more comprehensive and robust. Additionally, further exploration of ferroptosis-related pathways is essential to refine the drug concentration thresholds for ferroptosis, accurately pinpointing the inflection points of drug concentration. This will provide a stronger theoretical foundation for the future clinical translation of ferroptosis drugs, unlocking their greater clinical potential.

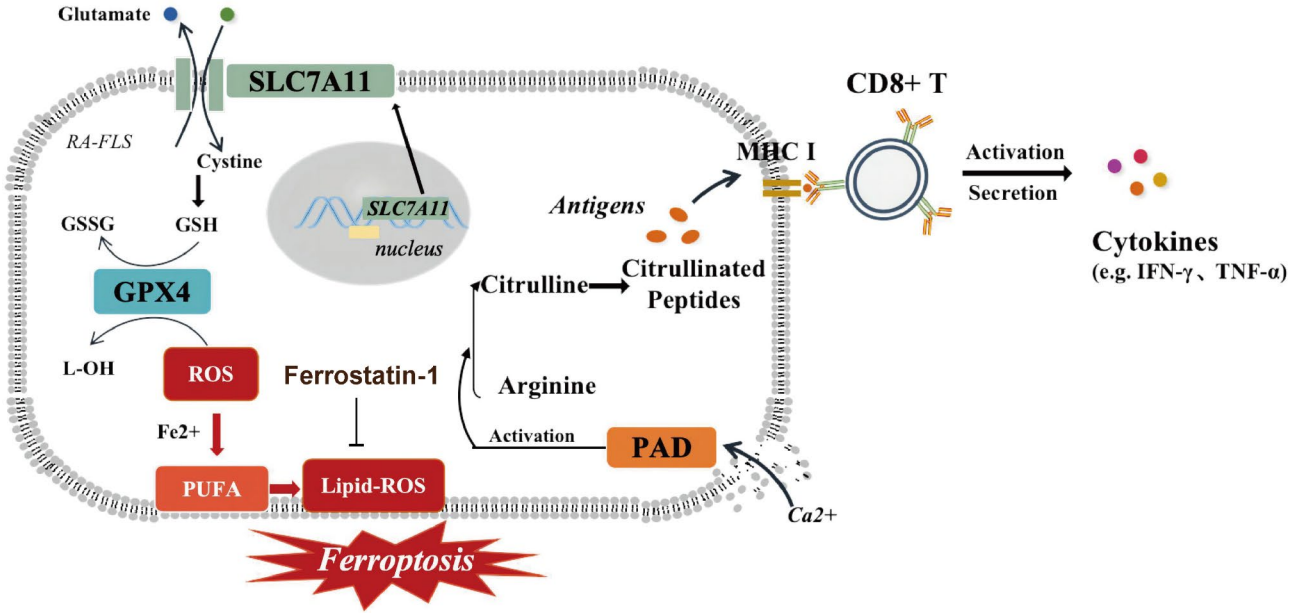

Fig. 6 Mechanism model of antigen-presenting effect of RA-FLSs induced by ferroptosis
The high level of ferroptosis in RA-FLSs causes the increase of intracellular PAD4 enzyme and citrullinated protein, which promote the function of endogenous antigen presenting and the aggregation of inflammatory factors. Ferrostatin-1 can inhibit the above reaction to achieve the therapeutic effect of RA

Conclusions

Ferroptosis can regulate the expression of cit-h3 in RA-FLSs through PAD4, thereby causing RA-FLSs to express high levels of HLA-I (MHC-I) molecules, triggering antigen presentation effects. Ferroptosis inhibitor can effectively reduce the antigen-presenting function of RA-FLSs and reduce inflammatory response. These findings suggest that ferroptosis plays a role in the inflammatory response in RA and ferroptosis inhibitors may be a new therapeutic approach for inhibiting the inflammatory response in RA (Fig. 6).

Supplementary Information

The online version contains supplementary material available at https://doi.org/10.1186/s12967-025-06300-0.

Supplementary Material 1

Acknowledgements

Thanks to Zhiyu Zhao for special help on organizing the data of this article.

Author contributions

XYZ, HYL, and ZYZ designed experiments; XYZ, HYL carried out experiments; HNJ, JWX, WJL, JZ, XMW, JYY, assisted in the experiments; XYZ, ZYZ, YLW, HYS collected clinical samples; XYZ, HYL, YLG analyzed experimental results; XYZ, HYL wrote the manuscript.

Funding

This work was supported by grants from the National Natural Science Foundation of China (82271826,81901638) and Outstanding Youth Medical Talents Foundation of the First Affiliated Hospital of Harbin Medical University (Grant No. 2021J07).

Data availability

The data that supports the findings of this study are available in the supplementary material of this article.

Declarations

Competing interest

No conflicts of interest were declared.

Received: 30 November 2024 / Accepted: 23 February 2025
Published online: 06 March 2025

References

1. Gravallese EM. Firestein. Rheumatoid arthritis - common origins, divergent mechanisms. N Engl J Med. 2023;388:529–42. https://doi.org/10.1056/NEJMra2103726.
2. Weyand CM, Goronzy JJ. The immunology of rheumatoid arthritis. Nat Immunol. 2021;22:10–8. https://doi.org/10.1038/s41590-020-00816-x.
3. Croft AP, Campos J, Jansen K, Turner JD, Marshall J, Attar M, et al. Distinct fibroblast subsets drive inflammation and damage in arthritis. Nature. 2019;570:246–51. https://doi.org/10.1038/s41586-019-1263-7.
4. Mizoguchi F, Slowikowski K, Wei K, Marshall JL, Rao DA, Chang SK, et al. Functionally distinct disease-associated fibroblast subsets in rheumatoid arthritis. Nat Commun. 2018;9:789. https://doi.org/10.1038/s41467-018-02892-y.
5. Tran CN, Davis MJ, Tesmer LA, Endres JL, Motyl CD, Smuda C, et al. Presentation of arthritogenic peptide to antigen-specific T cells by fibroblast-like synoviocytes. Arthritis Rheumatol. 2007;56:1497–506. https://doi.org/10.1002/art.22573.
6. Cho ML, Yoon CH, Hwang SY, Park MK, Min SY, Lee SH, et al. Effector function of type II collagen-stimulated T cells from rheumatoid arthritis patients: cross-talk between T cells and synovial fibroblasts. Arthritis Rheumatol. 2004;50:776–84. https://doi.org/10.1002/art.20106.
7. Lin J, Zhou Z, Huo R, Xiao L, Ouyang G, Wang L, et al. Cyr61 induces IL-6 production by fibroblast-like synoviocytes promoting Th17 differentiation in rheumatoid arthritis. J Immunol. 2012;188:5776–84. https://doi.org/10.4049/jimmunol.1103201.

8. Mondal S, Thompson PR. Protein arginine deiminases (PADs): biochemistry and chemical biology of protein citrullination. Acc Chem Res. 2019;52:818–32. https://doi.org/10.1021/acs.accounts.9b00024.
9. Fert-Bober J, Darrah E, Andrade F. Insights into the study and origin of the citrullinome in rheumatoid arthritis. Immunol Rev. 2020;294:133–47. https://doi.org/10.1111/imr.12834.
10. Alghamdi M, Alasmari D, Assiri A, Mattar E, Aljaddawi A A., Alattas S. G., et al. An overview of the intrinsic role of citrullination in autoimmune disorders. J Immunol Res. 2019;2019(7592851). https://doi.org/10.1155/2019/7592851.
11. Jiang X, Stockwell BR. Conrad. Ferroptosis: mechanisms, biology and role in disease. Nat Rev Mol Cell Biol. 2021;22:266–82. https://doi.org/10.1038/s41580-020-00324-8.
12. Dixon SJ, Lemberg KM, Lamprecht MR, Skouta R, Zaitsev EM, Gleason CE, et al. Ferroptosis: an iron-dependent form of nonapoptotic cell death. Cell. 2012;149:1060–72. https://doi.org/10.1016/j.cell.2012.03.042.
13. Fang X, Wang H, Han D, Xie E, Yang X, Wei J et al. Ferroptosis as a target for protection against cardiomyopathy. Proc. Natl. Acad. Sci. U. S. A., (2019); 116: 2672-80https://doi.org/10.1073/pnas.1821022116
14. Chen X, Kang R, Kroemer G, Tang D. Broadening horizons: the role of ferroptosis in cancer. Nat Rev Clin Oncol. 2021;18:280–96. https://doi.org/10.1038/s41571-020-00462-0.
15. Sanz AB, Sanchez-Niño MD, Ramos AM, Ortiz A. Regulated cell death pathways in kidney disease. Nat Rev Nephrol. 2023;19:281–99. https://doi.org/10.1038/s41581-023-00694-0.
16. Yu Y, Su Y, Yang S, Liu Y, Lin Z, Das NK, et al. Activation of intestinal HIF2α ameliorates iron-refractory anemia. Adv Sci. 2024;11:e2307022. https://doi.org/10.1002/advs.202307022.
17. Chen X, Kang R, Kroemer G, Tang D. Ferroptosis in infection, inflammation, and immunity. J Exp Med. 2021;218. https://doi.org/10.1084/jem.20210518.
18. Xiao Q, Yan L, Han J, Yang S, Tang Y, Li Q, et al. Metabolism-dependent ferroptosis promotes mitochondrial dysfunction and inflammation in CD4(+) T lymphocytes in HIV-infected immune non-responders. EBioMedicine. 2022;86:104382. https://doi.org/10.1016/j.ebiom.2022.104382.
19. Mu Q, Chen L, Gao X, Shen S, Sheng W, Min J, et al. The role of iron homeostasis in remodeling immune function and regulating inflammatory disease. Sci Bull. 2021;66:1806–16. https://doi.org/10.1016/j.scib.2021.02.010.
20. Aletaha D, Neogi T, Silman AJ, Funovits J, Felson DT, Bingham CO. 2010 Rheumatoid arthritis classification criteria: an American college of rheumatology/european league against rheumatism collaborative initiative. Arthritis Rheumatol. 2010;62:2569–81. https://doi.org/10.1002/art.27584. 3rd et al.
21. Altman R, Alarcón G, Appelrouth D, Bloch D, Borenstein D, Brandt K, et al. The American college of rheumatology criteria for the classification and reporting of osteoarthritis of the hip. Arthritis Rheumatol. 1991;34:505–14. https://doi.org/10.1002/art.1780340502.
22. Zhang J, Zhang Y, Ma Y, Luo L, Chu M, Zhang Z. Therapeutic potential of Exosomal circrna derived from synovial mesenchymal cells via targeting circEDIL3/miR-485-3p/PIAS3/STAT3/VEGF functional module in rheumatoi arthritis. Int J Nanomed. 2021;16:7977–94. https://doi.org/10.2147/ijn.S333465.
23. Zhang J, Ma Y, Zhang Y, Niu S, Chu M, Zhang Z. Angiogenesis is inhibited by arsenic trioxide through downregulation of the circHIPK3/miR-149-5p/FOXO1/VEGF functional module in rheumatoid arthritis. Front Pharmacol. 2021;12:751667. https://doi.org/10.3389/fphar.2021.751667.
24. Luo X, Chen Y, Lv G, Zhou Z, Chen J, Mo X, et al. Adenovirus-mediated small interfering RNA targeting TAK1 ameliorates joint inflammation with collagen-induced arthritis in mice. Inflammation. 2017;40:894–903. https://doi.org/10.1007/s10753-017-0534-4.
25. Lewis JS, Hembree WC, Furman BD, Tippets L, Cattel D, Huebner JL, et al. Acute joint pathology and synovial inflammation is associated with increased intra-articular fracture severity in the mouse knee. Osteoarthritis Cartilage. 2011;19:864–73. https://doi.org/10.1016/j.joca.2011.04.011.
26. Chu CQ. Fibroblasts in rheumatoidarthritis. N Engl J Med. 2020;383(1679–81). https://doi.org/10.1056/NEJMcibr2024718.
27. Nygaard G, Firestein GS. Restoring synovial homeostasis in rheumatoid arthritis by targeting fibroblast-like synoviocytes. Nat Rev Rheumatol. 2020;16:316–33. https://doi.org/10.1038/s41584-020-0413-5.
28. Okada Y, Wu D, Trynka G, Raj T, Terao C, Ikari K, et al. Genetics of rheumatoid arthritis contributes to biology and drug discovery. Nature. 2014;506:376–81. https://doi.org/10.1038/nature12873.
29. Firestein GS, McInnes IB. Immunopathogenesis of rheumatoid arthritis. Immunity. 2017;46:183–96. https://doi.org/10.1016/j.immuni.2017.02.006.
30. Scherer HU, Häupl T, Burmester GR. The etiology of rheumatoid arthritis. J Autoimmun. 2020;110:102400. https://doi.org/10.1016/j.jaut.2019.102400.
31. Raychaudhuri S, Sandor C, Stahl EA, Freudenberg J, Lee HS, Jia X, et al. Five amino acids in three HLA proteins explain most of the association between MHC and seropositive rheumatoid arthritis. Nat Genet. 2012;44:291–6. https://doi.org/10.1038/ng.1076.
32. van Delft MAM, Huizinga TWJ. An overview of autoantibodies in rheumatoid arthritis. J Autoimmun. 2020;110:102392. https://doi.org/10.1016/j.jaut.2019.102392.
33. Burkhardt H, Sehnert B, Bockermann R, Engström A, Kalden JR, Holmdahl R. Humoral immune response to citrullinated collagen type II determinants in early rheumatoid arthritis. Eur J Immunol. 2005;35:1643–52. https://doi.org/10.1002/eji.200526000.
34. Peng W, Wu S, Wang W. Correlation of serum citrullinated histone H3 levels with disease activity in patients with rheumatoid arthritis. Clin Exp Rheumatol. 2023;41:1792–800. https://doi.org/10.55563/clinexprheumatol/i3bcss.
35. Yan B, Ai Y, Sun Q, Ma Y, Cao Y, Wang J, et al. Membrane damage during ferroptosis is caused by oxidation of phospholipids catalyzed by the oxidoreductases POR and CYB5R1. Mol Cell. 2021;81:355–69. https://doi.org/10.1016/j.molcel.2020.11.024.
36. Wagh V, Doss MX, Sabour D, Niemann R, Meganathan K, Jagtap S, et al. Fam40b is required for lineage commitment of murine embryonic stem cells. Cell Death Dis. 2014;5:e1320. https://doi.org/10.1038/cddis.2014.273.
37. Yao X, Sun K, Yu S, Luo J, Guo J, Lin J, et al. Chondrocyte ferroptosis contribute to the progression of osteoarthritis. J Orthop Transl. 2021;27:33–43. https://doi.org/10.1016/j.jot.2020.09.006.
38. Wu J, Feng Z, Chen L, Li Y, Bian H, Geng J, et al. TNF antagonist sensitizes synovial fibroblasts to ferroptotic cell death in collagen-induced arthritis mouse models. Nat Commun. 2022;13:676. https://doi.org/10.1038/s41467-021-27948-4.
39. Zhao C, Sun G, Li Y, Kong K, Li X, Kan T, et al. Forkhead box O3 attenuates osteoarthritis by suppressing ferroptosis through inactivation of NF-κB/MAPK signaling. J Orthop Transl. 2023;39:147–62. https://doi.org/10.1016/j.jot.2023.02.005.
40. Curran AM, Naik P, Giles JT, Darrah E. PAD enzymes in rheumatoid arthritis: pathogenic effectors and autoimmune targets. Nat Rev Rheumatol. 2020;16:301–15. https://doi.org/10.1038/s41584-020-0409-1.
41. Halvorsen EH, Pollmann S, Gilboe IM, van der Heijde D, Landewé R, Ødegård S, et al. Serum IgG antibodies to peptidylarginine deiminase 4 in rheumatoid arthritis and associations with disease severity. Ann Rheum Dis. 2008;67:414–7. https://doi.org/10.1136/ard.2007.080267.
42. Harris ML, Darrah E, Lam GK, Bartlett SJ, Giles JT, Grant AV, et al. Association of autoimmunity to peptidyl arginine deiminase type 4 with genotype and disease severity in rheumatoid arthritis. Arthritis Rheumatol. 2008;58:1958–67. https://doi.org/10.1002/art.23596.
43. Darrah E, Giles JT, Davis RL, Naik P, Wang H, Konig MF, et al. Autoantibodies to peptidylarginine deiminase 2 are associated with less severe disease in rheumatoid arthritis. Front Immunol. 2018;9:2696. https://doi.org/10.3389/fimmu.2018.02696.
44. Damgaard D, Bawadekar M, Senolt L, Stensballe A, Shelef MA, Nielsen CH. Relative efficiencies of peptidylarginine deiminase 2 and 4 in generating target sites for anti-citrullinated protein antibodies in fibrinogen, alpha-enolase and histone H3. PLoS ONE. 2018;13:e0203214. https://doi.org/10.1371/journal.pone.0203214.
45. Blachère NE, Parveen S, Frank MO, Dill BD, Molina H, Orange DE. High-titer rheumatoid arthritis antibodies preferentially bind fibrinogen citrullinated by peptidylarginine deiminase 4. Arthritis Rheumatol. 2017;69:986–95. https://doi.org/10.1002/art.40035.
46. Liu X, Arfman T, Wichapong K, Reutelingsperger CPM, Voorberg J. Nicolaes. PAD4 takes charge during neutrophil activation: impact of PAD4 mediated NET formation on immune-mediated disease. J Thromb Haemostasis. 2021;19:1607–17. https://doi.org/10.1111/jth.15313.
47. Blachère NE, Parveen S, Fak J, Frank MO. Orange. Inflammatory but not apoptotic death of granulocytes citrullinates fibrinogen. Arthritis Res Ther. 2015;17:369. https://doi.org/10.1186/s13075-015-0890-0.
48. Valesini G, Gerardi MC, Iannuccelli C, Pacucci VA, Pendolino M, Shoenfeld Y. Citrullination and autoimmunity. Autoimmun Rev. 2015;14:490–7. https://doi.org/10.1016/j.autrev.2015.01.013.

49. Alghamdi M, Al Ghamdi KA, Khan RH, Uversky VN, Redwan EM. An interplay of structure and intrinsic disorder in the functionality of peptidylarginine deiminases, a family of key autoimmunity-related enzymes. Cell Mol Life Sci. 2019;76:4635–62. https://doi.org/10.1007/s00018-019-03237-8.

Publisher's note